# Interrelationship between atomic species, bias voltage, texture and microstructure of nano-scale multilayers

LEWIS, D.B., LUO, Q. <http://orcid.org/0000-0003-4102-2129>, HOVSEPIAN, P. E. <http://orcid.org/0000-0002-1047-0407> and MUNZ, W.D.

# Interrelationship between atomic species, bias voltage, texture and microstructure of nano-scale multilayers

D.B. Lewis*, Q. Luo, P.Eh. Hovsepian, W.-D. Munz

Materials Research Institute, Sheffield Hallam University, S1 1WB UK

**Abstract:** A matrix of binary and ternary nitrides containing lighter elements (Al, Ti, V and Cr) with atomic mass <52 and heavier elements (Nb and W) with atomic mass >89 has been formulated. These have been grown as nano-scale multilayer coatings (bilayer thickness approx. 3.0 nm) on stainless steel substrates using an industrial size multiple-target ABS coater. When lighter elements are incorporated into the multilayer at a lower bias voltage (UB = -75 V) pronounced {111} or {110}, textures develop which are determined by the dominating species present. A {111} or {110} texture develops when TiAlN or VN and or CrN dominates the matrix, respectively. In contrast when a heavier element is incorporated a {100} texture is observed. Additionally, there is a strong indication that in the case when heavy elements (>89) are involved in the growth process, which evolves by continuous re-nucleation. Conversely, when only light elements (<52) are involved then the coating evolves by competitive growth. This observation is limited only for the lower bias voltage range of UB -75 to -120 V. However, as the bias voltage is increased (up to UB = -150 V) the texture becomes increasingly sharp and in all cases a {111} texture develops. A lower residual compressive stress (typically -1.8 GPa) is observed when one of the bi-layers is dominated by a heavier element. The stress increases (up to -6.8 GPa) in these coatings when the bias voltage is increased to UB = -150 V which is always systematically lower than in coatings containing only lighter elements which are typically up to -11.7 GPa at the same bias voltage. In parallel this results in an increase in plastic hardness (80 GPa) and in the sliding wear coefficient by an order of magnitude regardless of the type of lattice growth observed.

**Keywords:** Texture; Residual stress; Atomic species; Magnetron sputtering; Structure evolution

## 1. Introduction

Early fundamental research on nano-scale multilayered hard coatings were conducted in the late 1980s,[1]. Based on this fundamental research on nano-scale multilayered hard coatings with hardness exceeding 50GPa were produced [2,3] and a number of TiN based nano-scale multilayered such as TiN/WN [4], TiN/CrN,TiN/TaN, TiN/MoN [5] and TiN/AlN [6] have been produced. Most of the coating systems were developed under laboratory conditions where PVD technologies such as magnetron sputtering and cathodic arc evaporation have been used to produce nano-scale multilayer structures [5–7]. However, the combined cathodic arc/unbalanced magnetron deposition method (Arc Bond Sputter, ABS) [8] has been used to grow successfully nano-scale multilayered coatings with highly reproducible structure in industrially sized PVD coaters [9–14].This article reports the interrelationship between atomic species, bias voltage, texture, residual stress and hardness of nano-scale multilayers deposited in an industrialised coater by the combined cathodic arc/unbalanced magnetron deposition method.

## 2. Experimental details

TiAlN/VN, TiAlN/CrN CrN/NbN and TiN/WN nano-scale multilayer coatings investigated were deposited by reactive unbalanced magnetron (UBM) sputtering in a Hauzer techno coating (HTC) 1000-4 using the Arc bond sputter process (ABS) [8]. This system comprises 4 vertically mounted targets that can be run in either a cathodic arc or an unbalanced magnetron(UBM) mode. The configurations used in this investigation are shown in Fig. 1 and are identified as cases 1–4. The deposition process used for nano-scale multilayer coatings is shown in Fig. 2. A chromium metal ion etch was used for the CrN/NbN and TiAlN/CrN coatings whereas TiAlN/VN and TiN/WN coatings were deposited after a V+ or Ti+ etch, respectively. This metal ion etch was used to

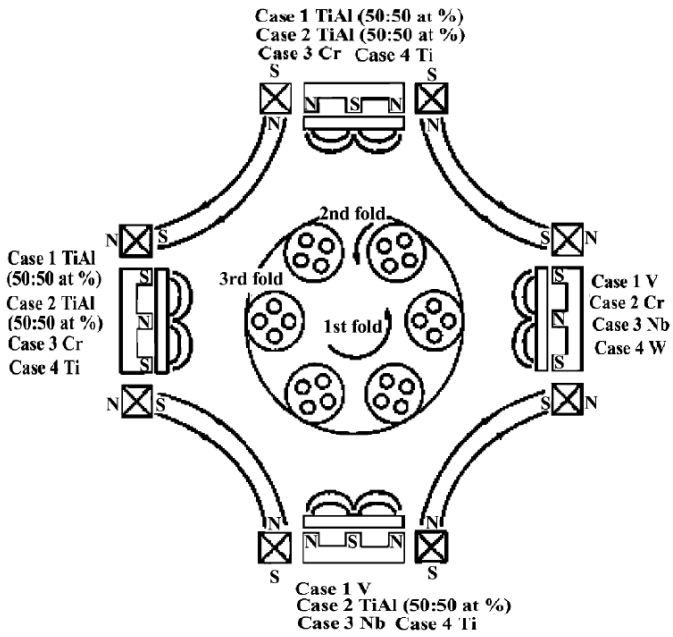


**Fig.** 1. Schematic diagram of the target arrangement used in the Hauzer HTC 1000-4 ABS™ PVD coating unit for the deposition of TiAlN/VN, TiAlN/CrN, CrN/NbN and TiN/WN nano-scale mulilayer films.

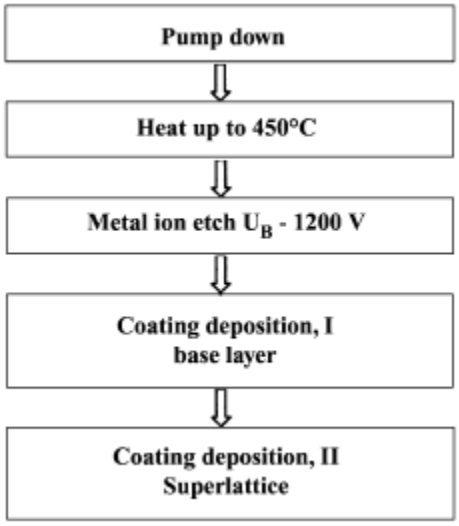


**Fig. 2.** The deposition process for nano-scale multilayer coatings.

enhance adhesion between coating and substrate. Following metal ion etching, a thin (0.3–0.5 mm) base layer was deposited by UBM sputtering to further improve adhesion. VN, CrN, and TiAlN were used as base layer materials prior to deposition of the nano-scale multilayer for the TiAlN/VN, CrN/NbN and TiAlN/CrN systems, respectively. The coatings were deposited at bias voltages between UB= -75 V and UB = -150 V using the target power shown in Table 1. All the coatings were deposited at a constant temperature of 450 □C in a common Ar+N2 atmosphere without shielding at a total pressure of 3.8x10-3 mbar. TiAlN/VN coatings were also deposited at total pressures of 4.5 and 5 x10-3 mbar at a bias voltage UB of -85 V. A more detailed description of the process parameters used are described elsewhere [9,11–14].

**Table 1** Target and power selection for various superlattice coatings

| System | Target no. | Power/Target |
|---|---|---|
| TiAlN/VN | 2 TiAl/2 V | 2×8 kW/2×6 kW (UBM) |
| TiAlN/CrN | 3 TiAl/1 Cr | 3×8 kW/1×8 kW (UBM) |
| CrN/NbN | 2 Cr/2 Nb | 2×5 kW/2×10 kW (UBM) |
| TiN/WN | 3 Ti/1 W | 3×8 kW/1×8 kW (UBM) |

Texture, T* was determined in accordance with the Harris inverse pole Figure technique [15].

$$T^* = \frac{\frac{I_{(hkl)}}{R_{(hkl)}}}{\left(\frac{1}{n}\right)\sum_0^n \frac{I_{(hkl)}}{R_{(hkl)}}} \quad (1)$$

where $I_{(hkl)}$ and $R_{(hkl)}$ are the intensities from the (hkl) reflections in the specimen and a random powder, respectively, and n is the number of reflections considered, i.e. 7. Thus, a T* value of unity signifies a random orientation, whilst for T* values greater than unity the plane is considered to have a preferred orientation. The bi-layer period of the nano-scale multilayer, D, was measured directly in the low angle region from the standard Bragg's equation [13]. Glancing angle parallel beam geometry was used to determine the state of residual stress present in the coatings [16]. For a thin film in a state of equibiaxial stress the equation describing the stress dependence of the lattice parameter, a is related by the equation:

$$a_\psi = \sigma a_0 \left\{\left[\frac{(1+\nu)}{E}\right]\sin^2\psi - \frac{2\nu}{E}\right\} + a_0 \quad (2)$$

where $a_0$ is the unstressed lattice parameter, E is the elastic modulus and n is the Poisson's ratio. For the Poisson's ratio, a value of 0.3 corresponding to that of TiN was used. The elastic modulus of each film was determined using a nano-indentation method. The stress can be determined from the slope of the least-squares fit of the plot of $a_\psi$ vs. $\sin^2\psi$.

The microstructure of the coatings was investigated by cross sectional transmission electron microscopy. The plastic hardness was measured using a Fischerscope. Pin-on-Disc measurements were made in dry sliding wear conditions using Al2O3 balls, a 5 N load at a linear speed of 0.1 m $s^{-1}$.

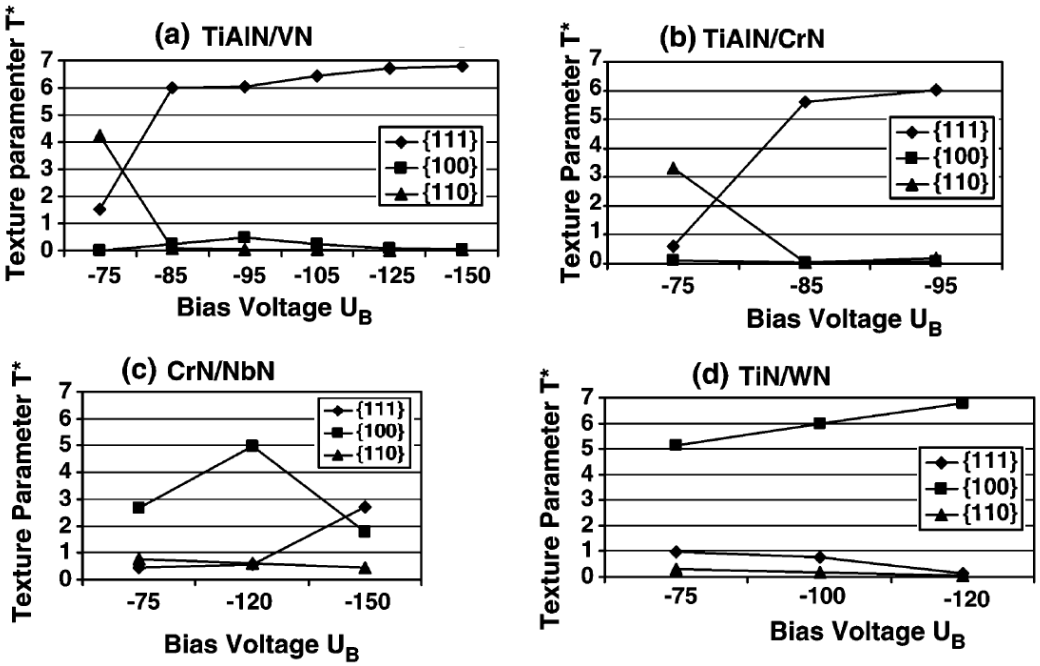

**Fig. 3.** (a) Effect of bias voltage, UB on texture development in TiAlNyVN Nano-scale Coatings, (b) Effect of bias voltage, UB on texture development in TiAlNyCrN Nano-scale Coatings, (c) Effect of bias voltage, UB on texture development in CrNyNbN Nano-scale Coatings, (d) Effect of bias voltage, UB on texture development in TiNyWN Nano-scale coatings.

## 3. Results and discussion

### 3.1. Texture development

The bi-layer periods of the nano-scale multilayers of the TiAlN/CrN, TiAlN/VN, CrN/NbN and TiN/WN coatings were between 3 and 3.5 nm. Fig. 3a–d show the effect of bias voltage UB on the texture development in TiAlN/VN, TiAlN/CrN, CrN/NbN and TiN/WN nano-scale multilayer coatings. From Fig. 3a–d it is clear that significant differences in texture were observed between films containing lighter elements, i.e. >52, e.g. TiAlN/VN and TiAlN/CrN compared with those containing heavier elements e.g. CrN/NbN and TiN/WN when deposited at a bias voltage UBsy75 V. The TiAlN/VN and TiAlN/CrN films exhibited a pronounced{110} texture whilst the CrN/NbN and TiN/WN films exhibited a {100} texture; see Fig. 3 a–d. In contrast where the TiAlN component in the TiAlN/CrN film is predominant a {111} texture develops (T* = 3.08). The presence of a {110} texture is common in high CrN containing films [13] where a process of competitive growth predominates. In fact strong {110} textures are present in magnetron sputtered monolithically grown CrN [17] and VN [18] films, grown under similar bias voltage conditions. This would indicate that at UB = -75 V the CrN or VN rich components were responsible for the development of {110} textures in TiAlN/CrN and TiAlN/VN coatings. Furthermore, the presence of a pronounced {111} texture (T* = 3.08) in TiAlN/CrN coatings, where the TiAlN component dominates, would lead one to the same conclusion. In contrast, the {100} texture develops when the surface energy becomes dominant [19] and the film evolves bya process of continuous re-nucleation. The latter effect is commonly observed in TiAlN systems where heavier atoms such as Nb [10] and Zr [20] are involved in the growth process.

For the TiAlN/VN and TiAlN/CrN films, increasing the substrate bias voltage to -85 V results in a pronounced change in texture from {110} at -75 V to strong {111} textures at -85 V (i.e. T* = 6.02 and 5.6,respectively). In the TiAlN/CrN and TiAlN/VN films, further increases in bias voltage UB = -95 V and UB = -150 V, respectively, lead to further increases in the intensity of the {111} texture, see Fig. 3 a,b. In contrast, increasing the bias voltage of the CrN/NbN and TiN/WN films to UB = -120 V did not favour the development of a {111} but in fact increased the intensity of the {100} texture. At a bias voltage of UB = -150 V at least for the CrN/NbN film, however, the {111} texture predominates.

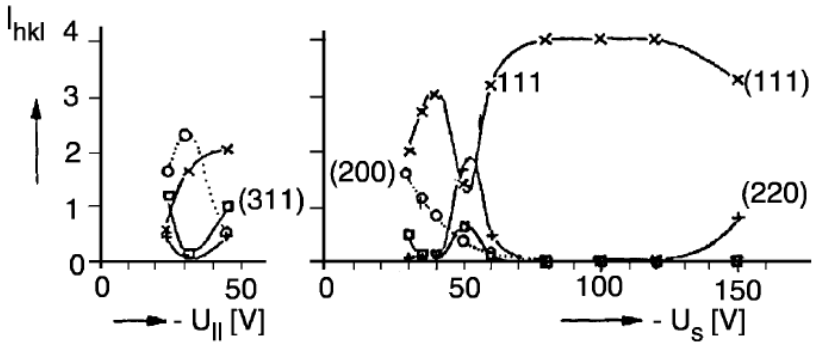


**Fig. 4**. Intensities {hkl} as a function of bias voltage [21].

Texture development in these nano-scale multilayer coatings follow the same trends as those observed by Kadlec et al. [21] in magnetron sputtered monolithic TiN coatings. A graph showing the intensity of reflections {hkl} vs. bias voltage from their work is included in Fig. 4 to aid the discussion. The TiAlN/VN and TiAlN/CrN coatings clearly follow the same trend as the magnetron sputtered TiN coatings, that is, a {110} texture followed by the development of a {111} texture, which increases in intensity with increasing bias voltage UB ($U_S$ in Fig. 4). In our investigation the {110} texture develops at UB = -75 V whereas in the TiN coating the {110} texture develops at UBsy50 V. One of the major effects of increasing bias voltage is that of increased adatom mobility. Therefore the exact relationship between bias voltage and texture is coating specific and will depend on such variables as coating species and deposition parameters, e.g. total pressure PT. One can therefore speculate that during deposition the order of textured development would be the same but the bias voltage at which specific textures develop are displaced to either higher or lower bias voltages depending on the coating species and deposition parameters. This is supported by our work, where similar TiAlN/VN nano-scale multilayer coatings have been deposited at higher total pressures PT at a bias voltage UB = -85 V, see Fig. 5. Increasing the

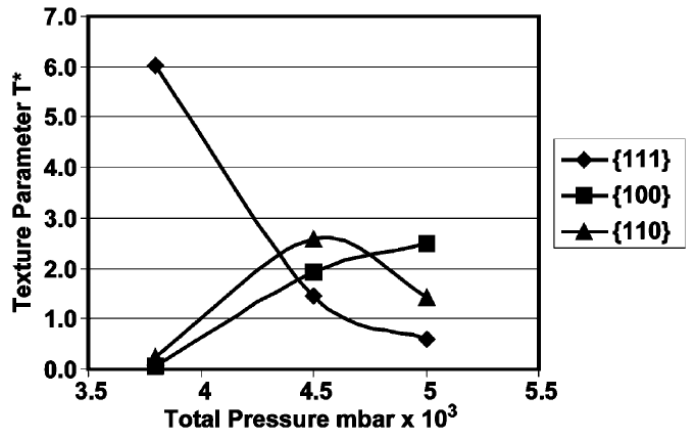


**Fig. 5.** Effect of total pressure $P_T$ on texture development in coatings deposited at UB = -85 V.

total pressure P from $3.8 \times 10^{-3}$ to $4.5 \times 10^{-3}$ mbar resulted in a texture change from {111} to {110}. Further increases in total pressure resulted in an increase in the {100} component. This is because at the same bias voltage increasing the total gas pressure PT decreases the energy of the bombarding ions and, therefore has a similar influence on texture formation as reducing the

bias voltage. Therefore the texture developed at UB= -85 V using a total pressure P = $4.5x10^{-3}$ mbar is similar to that developed at UB = -75 V using a total pressure P = $3.8x10^{-3}$ mbar, that is, a {110} texture Tin both cases. In our work increasing the total pressure has displaced the position of intensity maximums to higher bias voltages such that at the same bias voltage UB = -85 V, the {111} texture is replaced first by the {110} texture, then the {100} texture.

Using the same argument for the coatings incorporating heavier atoms, it is well established that under the same deposition conditions, the ad-atom mobility of the heavier atoms (Nb and W, >52) is systematically slower than that of the lighter more mobile lighter atoms (Al, Ti, V, and Cr-52). It can be therefore speculated that when heavier atoms are incorporated into the growing film, the curves showing the dependency of texture on bias voltage as shown in Fig. 4, are displaced to higher bias voltages. Therefore CrN/NbN and TiN/WN coatings at bias voltages, UB between -75 and -120 V are deposited in a regime where the {100} texture develops (i.e. conditions similar to those at bias voltage $U_S$ = -24 V in Fig. 4 ($I_{\{100\}}/I_{\{111\}} = 5$) [21]). The effect of less mobile elements on texture development can be supported by previous work on TiAlCrN based coatings deposited at UB = -75 V, where the non-uniform incorporation of only 2 at.% of the less mobile element, Y, resulted in a change from a {111} to a {100} texture [24,25]. In CrN/NbN coatings only at bias voltages of UB = -150 V did the films grow in a regime where a mixed {111} and {100} could develop (i.e. in conditions similar to those at bias voltage $U_S$> -30 V in Fig. 4).

### *3.2. Transmission electron microscopy*

Figs. 6 a–c show bright field / dark field typical transmission electron micrographs from a CrN/NbN coating deposited at UB = -120 V with the dark field images showing adjacent {100} (b) and {111} oriented grains(bright regions) (c). In Fig. 6b there is some evidence of continuous re-

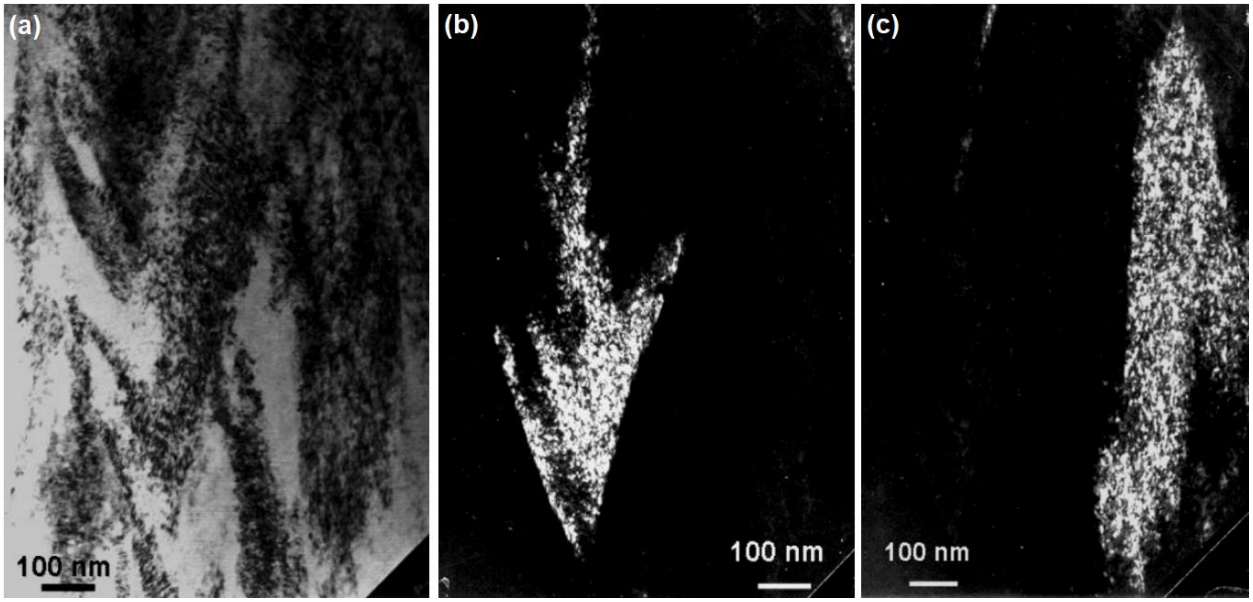

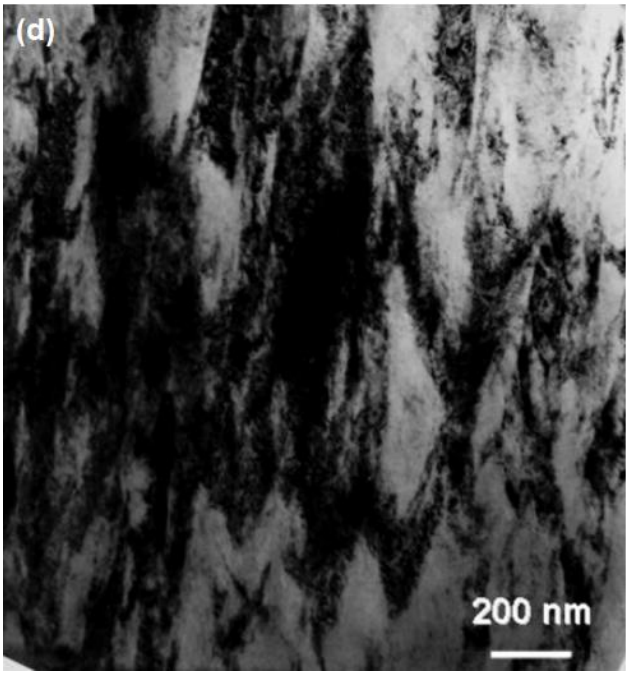


**Fig. 6. (a–c)** Transmission electron micrographs of CrN/NbN deposited at $U_B$ = -120 V: (a) Bright field image, (b) Dark field image from {200} diffraction ring segment, (c) Dark Field Image from {111} diffraction ring segment, Fig. 4 (d) Transmission electron micrographs of TiAlN/VN deposited at $U_B$ = -95 V, Bright field image.

nucleation of new {100} oriented grains which are growing at the expense of the {111} oriented grain shown in Fig. 4c, thus resulting in the formation of the {100} observed by X-ray diffraction.

In contrast the TiAlN/VN film in Fig. 6d evolved by a process of competitive columnar growth and selected area diffraction patterns showed that the pre-dominant growth direction was <111>, which is in agreement with the strong {111} texture (T* = 6.05) measured by X-ray diffraction.

Texture evolution w19x can be discussed on the basis of both surface and strain energies. Thus, for TiN and other fcc nitrides, because the {100} plane has the highest packing density (4.0 at/$a^2$ compared with {220}2.83 at/$a^2$ and {111} 2.31 at/$a^2$) and hence the lowest surface free energy [22,23], the {100} texture would develop when the surface energy is the dominant parameter [19]. Conversely, when the strain energy is the dominant the texture tends towards the {111} plane, which has the lowest strain energy. In very thin films the surface energy controls the growth so a {100} texture would be expected, whereas in thicker films the strain energy predominates and hence a {111} texture would be expected. In the TiAlN/VN nano-scale multilayer films the coatings evolved by a competitive columnar growth process, which after sufficient growth favours the development of a {111} texture [22]. In the competitive growth process, as the layer thickness increases the {111} texture develops because the {111} oriented grains with the lowest strain energy grow and increase in diameter at the expense of other less favourable orientations with a higher strain energy, e.g. {100}. In the micrograph of Fig. 4d there is clear evidence of coarsening of the structure by competitive growth. In contrast the CrN/NbN films deposited at bias voltages up to UB = -120 V the coating evolved by a continuous re-nucleation of new grains rather than by competitive growth of existing grains resulting in the development of a {100} texture (see Fig. 6b).

Nano-scale multilayer coatings can be considered to consist of individual layers of binary or ternary nitrides. In the case of heavier atoms Nb and W these are relatively immobile, even at bias voltages UB = -120V. Thus, the immobile layers of Nb and W atoms in the WN and NbN rich layers interrupts the columnar growth causing repeated formation of new nuclei and, therefore the texture develops as for very thin films where the surface energy is dominant and, therefore favours the development of a {100} texture. This type of growth has been observed in TiAlCrYN films, which develop a {100} texture when only 2 at.% of the lower mobility element Y is incorporated non-uniformly into a TiAlCrN coating [24]. Under similar deposition conditions, Y free TiAlCrN coatings develop a {111} texture and evolves by a process of competitive growth. Increasing the bias voltage UB to -150 V increases the mobility of the all atoms and, therefore less interruption of columnar growth resulting in the formation of a mixed {111}/{100} texture in CrN/NbN films deposited at UB = -150 V.

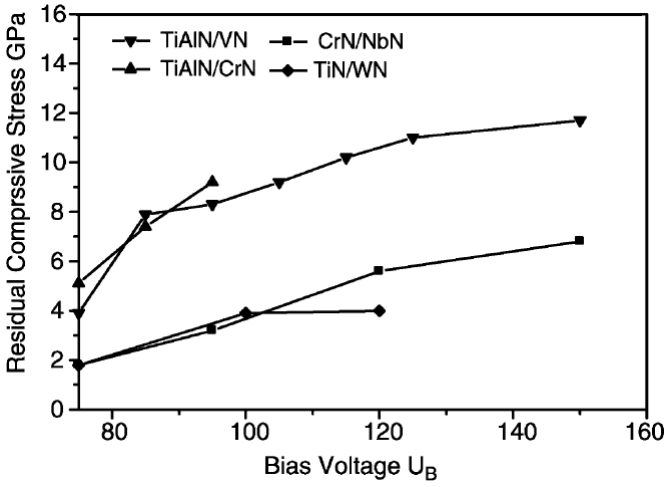


**Fig. 7.** Effect of bias voltage on the residual stress of ABS deposited nano-scale coatings.

### *3.3. Residual stress and plastic hardness*

Residual stress values for TiAlN/CrN, TiAlN/VN, CrN/NbN and TiN/WN films as a function of bias voltage UB are shown in Fig. 7. All the coatings investigated exhibited residual compressive stress states. However, at UB = -75 volts the TiAlN based systems nano-scaled multilayer coatings containing VN and CrN have a considerably higher residual stresses of -3.9 GPa and -5.0 GPa, respectively, when compared with CrN/NbN and TiN/WN nano-scaled multilayer coatings, which have a comparably low residual stress values of -1.8 GPa. This clearly indicates that where one of the components of the bi-layer is dominated by a heavy element a lower residual stress is observed. It is generally accepted that higher residual stresses are associated with higher defect densities induced during ion bombardment [10]. In UBM deposited coatings the dominant bombarding specie is Ar+ ion. Two of the many processes occurring simultaneously during ion bombardment are energy transfer to the condensing atoms and defect formation during coating growth. One possible explanation for the systematically lower residual stress observed in CrN/NbN and TiN/WN coatings is that higher activation energies are required for surface diffusion of less mobile heavier atoms (Nb and W, >52) than for more mobile lighter atoms (Al, Ti, V, and Cr <52).

For coatings involving heavy atoms, considering the energy conservation issue during deposition, at the same bias voltage, less energy is available for defect formation because a larger part of the energy is spent in moving atoms to their equilibrium position. In this case, a smaller portion of the total energy will be available for defect formation and, therefore a lower residual stress in the coating will be produced. An example of this effect can be demonstrated in CrN/NbN and TiN/WN coating systems where the maximum stress measured at UB = -75 V is only -1.8 GPa. Further increases in bias voltage up to UB = -150 V for the CrN/NbN nanoscale multilayer led to a systematic increase in the residual stress to a value of -6.8 GPa. In contrast the residual stress for the TiN/WN nano-scale multilayer containing the heavier element W increased to only 4GPa when the bias voltage, UB was increased to -120V.

In the case of the TiAlN/VN coatings, where only light elements (atomic mass <52) are involved, increases in the bias voltage, UB to -125 V and -150 V lead to residual stresses of -11.0 GPa and -11.7 GPa, respectively. These are almost greater by a factor 2 and 3, respectively, than the CrN/NbN and TiN/WN coatings deposited at similar bias voltages. These increases in residual stress can obviously be associated with increases in defect densities resulting from increases inthe energy portion available for defect formation in with increasing negative bias voltage. Plastic hardness values for TiAlN/VN and CrN/NbN films as a function of bias voltage UB are shown in Fig.8. The trends in the plastic hardness almost exactly mirror those of the respective residual stress in the selected coatings. However, the hardness of the TiAlN/VN coating was much harder than that of the CrN/NbN coating. It is well established that increases in residual stresses lead to higher hardness. Therefore one possible explanation for the higher hardness in the TiAlN/VN coating is that the residual stress in this coating is always systematically higher than that in the CrN/NbN coating at the same bias voltage.

### *3.4. Tribological tests*

Tribological test results for the CrN/NbN, TiAlN/CrN and TiAlN/VN coating deposited at different bias voltages, UB are shown in Table 2. In this work the TiAlN/VN system showed the lowest friction coefficient in dry sliding wear conditions ($\mu = 0.5$) and dry sliding wear coefficient ($K = 5.0 \times 10^{-17}$ $m^{-2}$ $N^{-1}$, which is 1 to 2 orders of magnitude less than the TiAlN/CrN and CrN/NbN

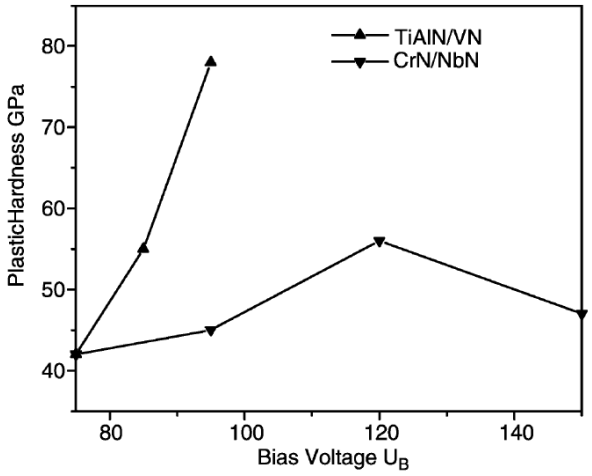


**Fig. 8.** Effect of bias voltage on the plastic hardness of ABS deposited nano-scale coatings.

**Table 2** Tribological results

| Specimen $/U_B$ | Coefficient of friction | Sliding wear $m^2N^{-1}$ | Specimen $/U_B$ | Coefficient of friction | Sliding wear $m^2N^{-1}$ |
|---|---|---|---|---|---|
| CrN/NbN − 75 V | 0.69 | 2.1 E-15 | TiAlN/VN − 75 V | 0.58 | 2.1 E-17 |
| CrN/NbN − 120 V | 0.9 | 5.0 E-15 | TiAlN/VN − 95 V | 0.56 | 5.0 E-17 |
| CrN/NbN − 150 V | 0.89 | 3.9 E-15 | TiAlN/VN − 125 V | 0.50 | 6.58 E-17 |
| TiAlN/CrN − 75 V | 0.7 | 2.38 E-16 | | | |
| TiAlN/CrN − 95V | 0.92 | 3.1 E-15 | | | |

coatings, respectively. For the TiAlN/CrN and CrN/NbN coatings the coefficient of friction and sliding wear resistance was found to be influenced by the residual stress, which was dependent on the bias voltage (UB). In all cases, increases in coefficients of friction and a reduction in dry sliding wear resistance can be correlated to increases in residual stress, which promote a brittle fracture mechanism [14]. In dry sliding wear fine debris (<1 mm in dia) is produced which results in 3 body tribological contact and a micro abrasive wear-mechanism. The type of product released depends on the coating system (V2O5 in TiAlN/VN,Cr2O3, CrNbO4 and Nb2O5 in CrN/NbN and TiO2 andCr2O3 in TiAlN/CrN) [14]. The lack of any dependence of residual stress on friction coefficient and lower friction coefficient for the TiAlN/VN coating results from the formation of a lubricious oxide (V2O5), which reduces the coefficient of friction.

## 4. Conclusions

1) Nano-scale multilayer coatings containing both light(< At Wt 52) and heavy elements (> At Wt 92)have been successfully deposited by the combined cathodic arc unbalanced magnetron sputtering method.
2) Where a heavy element is incorporated into the nanoscale multilayer then a {100} texture predominates, whereas when light elements only are present then a {111} texture predominates.
3) Increases in bias voltage leads to an increase in the intensity of the {111} texture, compressive stress and hardness.

4) When heavy elements are incorporated into the film then a systematically lower (1–1.8 GPa compared with 3.5–4.5 GPa) residual compressive stress is observed.
5) Residual stress influences the tribological properties of the coatings, increasing the friction coefficient and reducing the sliding wear resistance of the coatings.

## References

[1] U. Helmersson, S. Todorova, S.A. Barnett, J.-E. Sundgren, L.C. Markert, J.E. Greene, J. Appl. Phys. 62 (1987) 481.
[2] X. Chu, M.S. Wong, W.D. Sproul, S.L. Rohde, S.A. Barnett, J. Vac. Sci. Technol., A 10 (1992).
[3] X. Chu, S.A. Barnett, M.S. Wong, W.D. Sproul, Surf. Coat. Technol. 57 (1993) 13.
[4] T. Hurkmans, T. Trinh, D.B. Lewis, J.S. Brooks, W.-D. Munz, Surf. Coat. Technol. 76–77 (1995) 159.
[5] M. Nordin, M. Larson, S. Hogmark, Surf. Coat. Technol. 106(1998) 234.
[6] M. Setoyama, A. Nakayama, M. Tanaka, N. Katagawa, T.Nomura, Surf. Coat. Technol. 86–87 (1996) 225.
[7] W.D. Sproul, Surf. Coat. Technol. 86–87 (1996) 170.
[8] W.-D. Mu¨nz, D. Schulze, F. Hauzer, Surf. Coat. Technol. 50 (1992) 169.
[9] L.A. Donohue, W.-D. Munz, D.B. Lewis, J. Cawley, T. Hurkmans, T. Trinh, et al., Surf. Coat. Technol. 93 (1997) 69.
[10] I. Petrov, P. Losbichler, D. Bergstrom, J.E. Greene, W.-D.Munz, T. Hurkmans, et al., Thin Solid Films 302 (1997) 179.
[11] P.Eh. Hovsepian, D.B. Lewis, W.-D. Munz, A. Rouzaud, P.Juliet, Surf. Coat. Technol. 116–119 (1999) 727.
[12] W.-D. Munz, D.B. Lewis, P.Eh. Hovsepian, C. Schonjahn, A.Ehiasarian, I.J. Smith, Surf. Eng. 17 (2001) 15.
[13] D.B. Lewis, I.P. Wadsworth, W.-D. Munz, R. Kuzel Jr, V. Valvoda, Surf. Coat. Technol. 116–119 (1999) 284.
[14] P.Eh. Hovesepian, D.B. Lewis, W.-D. Munz, Surf. Coat. Technol.133–134 (2000) 166.
[15] G.B. Harris, Phil. Mag. 43 (1952) 113.
[16] D.E. Geist, A.J. Perry, J.R. Treglio, V. Valvoda, D. Rafaja, Adv. X-Ray Anal. 38 (1995) 471.
[17] T. Hurkmans, D.B. Lewis, H. Paritong, J.S. Brooks, W.-D.Munz, Surf. Coat. Technol. 114 (1999) 52.
[18] G. Farges, E. Beuprez, M.C. Staine-Catherine, Surf. Coat. Technol. 54–55 (1992) 115.
[19] J. Pelleg, L.Z. Zevin, S. Lungo, Thin Solid Films 197 (1991)117.
[20] I. Wadsworth, D.B. Lewis, G. Williams, J. Mater. Sci. 31 (1996) 5907.
[[21] S. Kadlec, J. Musil, V Valvoda, W.-D. Munz, H. Petersein, J.Schroeder, Vacuum 41 (1990) 2238.
[22] L. Hultman, J.-E. Sundgren, J.E. Greene, J. Appl. Phys. 66(1989) 536.

[23] J.E. Greene, J.-E. Sundgren, L. Hultman, I. Petrov, D.B. Bergstrom, Appl. Phys. Lett. 67 (1995) 2928.

[24] L.A. Donohue, I.J. Smith, W-.D Munz, I. Petrov, J.E. Greene, Surf. Coat. Technol. 94y95 (1997) 226.

[25] D.B. Lewis, L.A. Donohue, M. Lembke, W.-D. Munz, R. KuzelJr, V. Valvoda, et al., Surf. Coat. Technol. 114 (1999) 187.